

Analyzing Predator-Prey Interaction in Chaotic and Bifurcating Environments

Ansar Abbas ^{*,1} and Abdul Khaliq ^{*,2}

*Department of Mathematics, Riphah International University, Lahore, Pakistan.

ABSTRACT An analysis of discrete-time predator-prey systems is presented in this paper by determining the minimum amount of prey consumed before predators reproduce, as well as by analyzing the system's stability and bifurcation. In order to investigate the local stability of the interior equilibrium point of the proposed model, discrete dynamics system theory is employed first. Moreover, the characteristic equation is analyzed to determine the Neimark-Sacker (NS) bifurcation of the system. The normal form and bifurcation theory are used to investigate the NS bifurcation around the interior equilibrium point. Based on its analysis, the system exhibits Neimark-Sacker bifurcation when positive parameters are present and non-negative conditions are met. The region of stability of chaotic behavior can be discovered by developing a feedback control strategy. By utilizing the maximum Lyapunov exponent, the effect of initial conditions on developed systems is further explored. Finally, a computer simulation illustrates the results of the analysis.

KEYWORDS

Lotka-volterra stability
Predator-Prey model
fixed points
Neimark-sacker bifurcation
Maximum lyapunov exponent
Chaos control

INTRODUCTION

It is widely known that predators and prey interact dynamically in nature, which helps to link complex food chains and food networks. The biological functions of predator-prey system dynamics have been explained by several predator-prey models. Predator-prey models are widely regarded as being one of the best, Lotka-Volterra is receiving increasing attention in recent years (R. M. Eide 2018; Pan 2013). Many studies have sought to understand the dynamical properties of the Lotka-Volterra model, since it plays an important role in ecosystem studies. These properties include dynamical behavior, stability, persistence, and antiperiodic, periodic, and near periodic solutions (Z. L. Luo 2016; X. W. Jiang 2021).

Natural interactions between predators and prey are fascinating puzzles. Ecology's fascination with ecosystems comes from the intimate interconnections between species. When chaos and bifurcation are introduced into this intricate dance, figuring out the dynamics becomes even more difficult. A chaotic environment characterized by sudden shifts and unpredictability complicates predator-prey relationships. An environment such as this is conducive to the development of novel patterns, unexpected results,

as well as a better understanding of the nature of life. The purpose of this study is to shed light on predator-prey interactions within chaotic and bifurcating environments, as well as their mechanisms, effects, and ecological implications. To understand these systems and reveal hidden connections, we will utilize chaos theory, mathematical modeling, and ecological studies (Zu *et al.* 2018; Q. 2015; Hu Z. 2011; Ibrahim and Touafek 2014; L. Men 2015).

In this exploration, we will draw on innovative research and seminal studies on predator-prey interactions. By examining the works of ecological pioneers like Lotka and Volterra, our scientific investigation will weave a rich tapestry. It is our goal to examine predator-prey relationships in environments that challenge conventional wisdom and our understanding of the natural world. This investigation will help us unravel the enigmatic language of life, which is enigmatic.

When it comes to population dynamical models, difference equation-based models and differential equation-based models can be distinguished from each other. Recent years have seen an increase in the popularity of discrete-time population models (Q. 2015; L. Men 2015). For the following reasons, discrete-time models are more appropriate than continuous-time models when populations have non-overlapping generations and small numbers of populations. The second reason is that discrete-time simulation results are more accurate. Moreover, continuous-time models can be numerically simulated by discretising and transforming them

Manuscript received: 8 September 2023,

Revised: 22 October 2023,

Accepted: 23 October 2023.

¹kute_ansar@yahoo.com (Corresponding Author)

²khaliqsyed@gmail.com

into its discrete counterpart. As a result, discrete-time models exhibit rich dynamical behaviors. In a study entitled Periodic Solution of Predator-Prey Models, (Fazly and Hesaaraki 2007; X. Zhang 2016), (Zhang C.H 2010) performed studies on periodic solutions to determine their stability, permanence, and existence. In discrete dynamical systems, properties such as periodicity, local and global stability, persistence, uniqueness of equilibrium, and boundedness of solutions are taken into account (Garic Demirovic M. 2009; Q. 2015; Kalabusic S. 2011; Ibrahim and Touafek 2014). Numerous articles also investigated the possibility of bifurcation and chaos when using discrete-time models (Hu Z. 2011; Sen M 2012; Chen and Changming 2008; Gakkhar and Singh 2012; Joydip Dhar 2015).

Smith et. al. (Smith 1968) introduced the following predator-prey model where U_n and V_n represent the prey and predator population sizes, respectively.

$$\left. \begin{aligned} U_{n+1} &= \left(R - \frac{U_n(R-1)}{U_E} - CV_n \right) U_n \\ V_{n+1} &= \frac{r}{U_E} U_n V_n \end{aligned} \right\} \quad (1)$$

Where, U_E represents the equilibrium density of preys in the absence of predator. R and r denote the maximum reproductive rates of the prey and predator respectively, C is a constant. Unfortunately, (Smith 1968) was unable to find the bifurcation parameter of the system (1) as well as the equilibrium point where the bifurcation exists. A modification to the predator-prey model is made by (Khan 2016) and is presented as follows:

$$\left. \begin{aligned} s_{n+1} &= \rho (1 - s_n) s_n - s_n t_n, \\ t_{n+1} &= \frac{1}{Y} s_n t_n \end{aligned} \right\} \quad (2)$$

where s_n and t_n represent the number of preys and predators, respectively. The initial values s_0, t_0 are positive real numbers while ρ, Y are parameters. In contrast to (Smith 1968), (Khan 2016) did not find out numerically the results of the Neimark-Sacker bifurcation for model (2) but discussed in an understandable manner all the theoretical aspects of the Neimark-Sacker bifurcation that has become an important topic.

In dynamical systems theory, Neimark-Sacker bifurcations are named after Russian mathematician L. A. Neimark and American mathematician A.F Shilnikov. Dynamic systems are characterized by the point at which a stable periodic orbit turns into chaos. As a result of this bifurcation, the system exhibits a complex, non-repeating behavior. Natural and engineered systems, such as weather patterns and electricity circuits, exhibit Neimark-Sacker bifurcations, which are fundamental to understanding chaos.

Based on (Smith 1968), we have developed a modified discrete predator-prey model that follows:

$$\left. \begin{aligned} x_{n+1} &= (1 - A)x_n^2 + x_n(A - y_n) \\ y_{n+1} &= \frac{1}{B}x_n y_n \end{aligned} \right\} \quad (3)$$

Biological description of parameters are mentioned in Table 1

Considering its structure, this paper can be separated into the following sections. In Section-2, we discuss how equilibria exists and how they are stable locally in R_2^+ for the system (3). Furthermore, our discussion focuses on the specific parametric conditions required for the existence of a Neimark-Sacker bifurcation. As

a bifurcation parameter A is used in Section-3 to study bifurcation (NS). By using feedback control methods, a stable region is achieved in section-4. The numerical simulations presented in Section-5 support the theoretical discussion. By showing the Maximum Laypnuov exponent in section-6, the fluctuation of the system is discussed according to its initial condition. Finally, we present a brief conclusion in Section-7.

EQUILIBRIUM POINTS AND THEIR STABILITY

The purpose of this section is to examine the existence of fixed points in discrete systems and analyses their stability. By using the formula given below, we can determine the fixed points of system (3) which satisfy

$$\left. \begin{aligned} x_n &= x_{n+1} = x^*, \\ y_n &= y_{n+1} = y^* \end{aligned} \right\}$$

When we use it in the model (3), we get the following result:

$$\left. \begin{aligned} x^* &= (1 - A)(x^*)^2 + x^*(A - y^*), \\ y^* &= \frac{1}{B}x^*y^* \end{aligned} \right\} \quad (a^*)$$

Framework (a*) clearly describes the fixed points of model (1).

(i) The system (3) has always a Extinction equilibrium point $E_1 = (0, 0)$.

(ii) The system (3) has Extinction and Exclusion equilibrium points $E_1 = (0, 0)$ and $E_2 = (1, 0)$ for $B < 1$.

(iii) There is a unique equilibrium point for the system (3) that is $E_3 = (B, A + (1 - A)B - 1)$ for $A < 1, B > 1$.

Our discussion now turns to the dynamics of model (1) about these equilibrium points. Linearized system (1) about fixed points (x, y) can be described by the Jacobian matrix

$$J(E_i) = \begin{pmatrix} A + 2(1 - A)x - y & -x \\ \frac{y}{B} & \frac{x}{B} \end{pmatrix}$$

as a result, the Jacobian matrix J of the linearized system (3) over the unique positive equilibrium $(B, A + (1 - A)B - 1)$ is defined by

$$\lambda^2 + r\lambda + s = 0 \quad (a^{**})$$

where, $r = AB - B - 2, s = A - 2AB + 2B$

Additionally, As can be seen from the equation above, all eigenvalues of the Jacobian of (3) evaluated at the unique positive equilibrium $(B, A + (1 - A)B - 1)$ are calculated as follows:

$$\lambda_{1,2} = \frac{1}{2}(2 + B - AB \pm \sqrt{\Delta})$$

where,

$$\Delta = r^2 - 4rs$$

Table 1 Description of the parameters

Parameter	Role in the Model
x_n	Prey population size at a particular time step.
y_n	Predator population size at a particular time.
A	Represents prey population intrinsic growth rate, which determines the reproduction rate of preys.
B	Measuring predator productivity in converting prey. When predators successfully consume their prey.

$$\Delta = -4(A + 2B - 2AB) + (-2 - B + AB)^2$$

As a means of analyzing how stable the fixed points of the model (3) are, here is the following definition:

Definition 1:

A fixed point (P, Q) is called

(i) a sink if $|\lambda_1| < 1$ and $|\lambda_2| < 1$, it is locally asymptotically stable.

(ii) when $|\lambda_1| > 1$ and $|\lambda_2| > 1$, the source is unstable.

(iii) if $|\lambda_1| < 1$ and $|\lambda_2| > 1$ or ($|\lambda_1| > 1$ and $|\lambda_2| < 1$), it is saddle.

(iv) if either $|\lambda_1| = 1$ or $|\lambda_2| = 1$, it is not hyperbolic. Using the definition above, we will derive the lemma (2.1) from the topological classification of the fixed points within the model (3). If we evaluate the dynamical map in (3) at any point (x, y) , Jacobian matrix is calculated as follows:

$$J(E_1) = \begin{pmatrix} A & 0 \\ 0 & 0 \end{pmatrix}$$

$$J(E_2) = \begin{pmatrix} 2 - A & -1 \\ 0 & \frac{1}{B} \end{pmatrix}$$

$$J(E_3) = \begin{pmatrix} 1 + B - AB & -B \\ \frac{-1 + A + B - AB}{B} & 1 \end{pmatrix}$$

Having discussed the models' fixed points (3), we will now discuss their topological classification. From (a**) we have:

Lemma 1: The following topological classification holds for the fixed point $E_1(0,0)$

(i) When $A < 1$ the point E_1 becomes sink .

(ii) When $A > 1$ the point E_1 is saddle .

(iii) When $A = 1$ the point E_1 is non-hyperbolic.

Lemma 2:

The following topological classification holds for the fixed point $E_2(1,0)$

(i) If $A > 1$ and $B > 1$ then $E_2(1,0)$ is a sink .

(ii) If $A < 1$ and $B > 1$ then $E_2(1,0)$ is a saddle .

(iii) If $A = 1$ or $B = 1$ then $E_2(1,0)$ will be non-hyperbolic .

Lemma 3:

The following topological classification holds for the fixed point

$$E_3 = (B, A + (1 - A)B - 1) \text{ for } A < 1, B > 1$$

(i) Among the following parametric conditions, E_3 is a sink if one of the following parametric conditions holds:

(i.a) $r \geq 4s$ and $0 < A < 1$

(i.b) $r < 4s$ and $A < (\frac{B-2}{B})^2$

(ii) It is possible for E_3 to be a source if one of the following parametric conditions holds:

(ii.a) $r \geq 4s$ and $A > 1$

(ii.b) $r < 4s$ and $A > (\frac{B-2}{B})^2$

(iii) When one parametric condition is satisfied, E_3 will not be hyperbolic if one of the following parametric conditions holds:

(iii.a) $r \geq 4s$ and $A = 1$

(iii.b) $r < 4s$ and $A = (\frac{B-2}{B})^2$

NEIMARK-SACKER BIFURCATION AT E_3

Using Lemma(2.3), E_3 cannot be hyperbolic when $A = 1$. The Neimark-Sacker bifurcation in the system (3) can therefore be studied by choosing A as the bifurcation parameter near the point E_3 . In this context, non-hyperbolic parameters are denoted as

$$H_k = \{ (A, B); \Delta < 0, A = (\frac{B-2}{B})^2, B > 1, A, B > 0 \}$$

Here's a description of the system (3) with arbitrary parameters $(\alpha, \beta) \in H_k$

$$\left. \begin{aligned} x_{n+1} &= (1 - \alpha)x_n^2 + x_n(\alpha - y_n), \\ y_{n+1} &= \frac{1}{\beta}x_n y_n \end{aligned} \right\} \quad (4)$$

One can easily found that the point $(\beta, \alpha + (1 - \alpha)\beta - 1)$ is the unique positive equilibrium point for the system (4) when $\beta > 1, \alpha < 1$. The following perturbations would be made to model (4)

$$\left. \begin{aligned} x_{n+1} &= (1 - (\alpha + \alpha_1))x_n^2 + x_n((\alpha + \alpha_1) - y_n), \\ y_{n+1} &= \frac{1}{\beta}x_n y_n \end{aligned} \right\} \quad (5)$$

where $|\alpha_1| \ll 1$, which is small parameter. Using (5) as a linearized system and $P_1(\beta, \alpha + (1 - \alpha)\beta - 1)$, as a unique point of positive equilibrium, the Jacobian matrix has the following characteristic equation:

$$\zeta^2 + r(\alpha_1)\zeta + s(\alpha_1) = 0$$

where,

$$r(\alpha_1) = (\alpha + \alpha_1)\beta - \beta - 2, \quad s(\alpha_1) = (\alpha + \alpha_1) - 2\alpha\beta + 2\beta$$

The characteristic equation, as well as the roots of the characteristic equation, change when α varies in a small radius around 0,

$$\zeta_{1,2} = \frac{-r(\alpha_1) \pm \sqrt{r^2(\alpha_1) - 4s(\alpha_1)}}{2}$$

$$\zeta_{1,2} = \frac{(\alpha + \alpha_1)\beta - \beta - 2 \pm \sqrt{((\alpha + \alpha_1)\beta - \beta - 2)^2 - 4((\alpha + \alpha_1) - 2\alpha\beta + 2\beta)}}{2}$$

$$\zeta_{1,2} = \frac{(\alpha + \alpha_1)\beta - \beta - 2 \pm \sqrt{((\alpha + \alpha_1)\beta - \beta - 2)^2 - 4((\alpha + \alpha_1) - 2\alpha\beta + 2\beta)}}{2}$$

For $\alpha_1 < \frac{2((s(\alpha_1))^{\frac{1}{2}} + 1) + \beta(1 - \alpha)}{\beta}$ there are two complex conjugate roots.

Also, we have

$$\text{tr}J(P_1) \neq 0, -1$$

$$\frac{d|\zeta_{1,2}|}{d\alpha_1} \Big|_{\alpha_1} = 4(\alpha\beta^2 - (\beta + 1)^2) > 0$$

After simplification we get $\zeta_{1,2}^i \neq 1$ for $i = 1, \dots, 4$, is satisfied.

A method for transforming the equilibrium point $P_1(\beta, \alpha + (1 - \alpha)\beta - 1)$ of the system (5) into its origin, we take $u_n = x_n - \beta$, $v_n = y_n - \alpha - (1 - \alpha)\beta + 1$. After calculation we get,

$$\left. \begin{aligned} u_{n+1} &= (1 - (\alpha + \alpha_1))(u_n + \beta)^2 + (u_n + \beta)((\alpha + \alpha_1) - (v_n + \alpha + (1 - \alpha)\beta - 1)) \\ v_{n+1} &= \frac{1}{\beta}(u_n + \beta)(v_n + \alpha + (1 - \alpha)\beta - 1) \end{aligned} \right\} \quad (6)$$

We examine system (5) in its normal form when $\alpha_1 = 0$ in the following way. The Taylor series at $(u_n, v_n) = (0, 0)$ is as follows:

$$\left. \begin{aligned} u_{n+1} &= b_{11}u_n + b_{12}v_n + b_{13}u_n^2 + b_{14}u_nv_n + b_{15}, \\ v_{n+1} &= b_{21}u_n + b_{22}v_n + b_{23}u_nv_n + b_{24} \end{aligned} \right\} \quad (7)$$

Where,

$$b_{11} = 1 - \beta - \alpha\beta, b_{12} = -\beta, b_{13} = -\alpha, b_{14} = -1, b_{15} = 1 + \beta - \beta^2$$

$$b_{21} = \frac{(1 - \alpha)(\beta - 1)}{\beta}, b_{22} = 1, b_{23} = \frac{1}{\beta}, b_{24} = (1 - \alpha)(\beta - 1)$$

The linear part of (7) is transformed into a canonical form by the matrix T

$$T = \begin{pmatrix} b_{12} & 0 \\ \mu - b_{11} & -\eta \end{pmatrix} \begin{pmatrix} X_n \\ Y_n \end{pmatrix}$$

where,

$$\mu = \frac{(\alpha + \alpha_1)\beta - \beta - 2}{2},$$

and

$$\eta = \frac{\sqrt{((\alpha + \alpha_1)\beta - \beta - 2)^2 - 4((\alpha + \alpha_1) - 2\alpha\beta + 2\beta)}}{2}.$$

In this way, the system (7) can be expressed as follows:

$$\left. \begin{aligned} X_{n+1} &= \mu X_n - \eta Y_n + \tilde{H}(X_n, Y_n) \\ Y_{n+1} &= \eta X_n + \mu Y_n + \tilde{K}(X_n, Y_n) \end{aligned} \right\} \quad (8)$$

where

$$\left. \begin{aligned} \tilde{H}(X_n, Y_n) &= m_{11}X_n^2 + m_{12}X_nY_n + m_{13} \\ \tilde{K}(X_n, Y_n) &= m_{21}X_n^2 + m_{22}X_nY_n + m_{23} \end{aligned} \right\} \quad (9)$$

and

$$m_{11} = b_{12}b_{13} + (\mu - b_{11})b_{14}, \quad m_{12} = -b_{14}\eta, \quad m_{13} = b_{15}$$

$$m_{21} = b_{12}b_{23}(\mu - \eta), \quad m_{22} = -b_{12}b_{23}\eta, \quad m_{23} = b_{24}$$

Furthermore,

$$\tilde{H}_{X_n X_n} |_{(0,0)} = 2m_{11}, \quad \tilde{H}_{X_n Y_n} |_{(0,0)} = m_{12}, \quad \tilde{H}_{Y_n Y_n} |_{(0,0)} = 0$$

$$\tilde{H}_{X_n X_n X_n} |_{(0,0)} = \tilde{H}_{X_n X_n Y_n} |_{(0,0)} = \tilde{H}_{X_n Y_n Y_n} |_{(0,0)} = \tilde{H}_{Y_n Y_n Y_n} |_{(0,0)} = 0$$

and

$$\tilde{K}_{X_n X_n} |_{(0,0)} = 2m_{21}, \quad \tilde{K}_{X_n Y_n} |_{(0,0)} = m_{22}, \quad \tilde{K}_{Y_n Y_n} |_{(0,0)} = 0$$

$$\tilde{K}_{X_n X_n X_n} |_{(0,0)} = \tilde{K}_{X_n X_n Y_n} |_{(0,0)} = \tilde{K}_{X_n Y_n Y_n} |_{(0,0)} = \tilde{K}_{Y_n Y_n Y_n} |_{(0,0)} = 0$$

For (8) to experience the Neimark-Sacker bifurcation, the following relation must be nonzero (Singh and Deolia 2020)

$$\Omega = -\text{Re} \left[\frac{(1 - 2\bar{\lambda})\bar{\lambda}^2}{1 - \bar{\lambda}} \zeta_{11}\zeta_{20} \right] - \frac{1}{2} \| \zeta_{11} \|^2 - \| \zeta_{02} \|^2 + \text{Re}(\bar{\lambda} \zeta_{21})$$

Where,

$$\zeta_{02} = \frac{1}{8} [\tilde{H}_{X_n X_n} - \tilde{H}_{Y_n Y_n} + 2\tilde{K}_{X_n Y_n} + \iota(\tilde{K}_{X_n X_n} - \tilde{K}_{Y_n Y_n} + 2\tilde{H}_{X_n Y_n})] |_{(0,0)},$$

$$\zeta_{11} = \frac{1}{4} [\tilde{H}_{X_n X_n} - \tilde{H}_{Y_n Y_n} + \iota(\tilde{K}_{X_n X_n} + \tilde{K}_{Y_n Y_n})] |_{(0,0)},$$

$$\zeta_{20} = \frac{1}{8} [\tilde{H}_{X_n X_n} - \tilde{H}_{Y_n Y_n} + 2\tilde{K}_{Y_n Y_n} + 2\tilde{K}_{X_n Y_n} + \iota(\tilde{K}_{X_n X_n} - \tilde{K}_{Y_n Y_n} - 2\tilde{H}_{X_n Y_n})] |_{(0,0)} \Lambda_1 \Lambda_2 = A + 2B - 2AB - p - \frac{(-1+A)(-1+B)q}{B} \quad (14)$$

$$\zeta_{21} = \frac{1}{16} [\tilde{H}_{X_n X_n X_n} + \tilde{H}_{X_n Y_n Y_n} + \tilde{K}_{X_n X_n Y_n} + \tilde{K}_{Y_n Y_n Y_n} + \iota(\tilde{K}_{X_n X_n X_n} + \tilde{K}_{X_n Y_n Y_n} - \tilde{H}_{X_n X_n Y_n} - \tilde{H}_{X_n X_n Y_n})] |_{(0,0)}$$

After calculation, we get

$$\zeta_{02} = \frac{1}{4} [m_{11} + m_{22} + \iota(m_{21} + m_{12})],$$

$$\zeta_{11} = \frac{1}{2} [m_{11} + \iota m_{21}],$$

$$\zeta_{20} = \frac{1}{4} [m_{11} + m_{22} + \iota(m_{21} - m_{12})],$$

$$\zeta_{21} = 0,$$

CHAOS CONTROL

The whole point of this section is to explore chaos control via state feedback control (Singh and Deolia 2020; Salman SM 2016; Alaydi 1996; Rana et al. 2017; Abarbanel 1996). To ensure that this section is comprehensive, we will first give an explanation of marginal stability.

Definition 2: Marginally stable refers to systems or processes that are neither stable nor unstable, but exist at the boundary between stability and instability. This indicates the possibility of an unstable system occurring when a small perturbation occurs.

In this case, we have a discrete biological model (3) that is as follows:

$$\left. \begin{aligned} x_{n+1} &= (1-A)x_n^2 + x_n(A-y_n) + w_n \\ y_{n+1} &= \frac{1}{B}x_n y_n \end{aligned} \right\} \quad (10)$$

Control is added by the addition of $w_n = -p(x_n - B) - q(y_n - (A + (1-A)B - 1))$, with p, q indicating feedback gains. At the interior fixed point P of the controlled system (10), the variational matrix V_P is evaluated according to the map below:

$$(F, G) \mapsto (x_{n+1}, y_{n+1}) \quad (11)$$

Where

$$\left. \begin{aligned} F : &= (1-A)x_n^2 + x_n(A-y_n) - p(x_n - B) - q(y_n - (A + (1-A)B - 1)) \\ G : &= \frac{1}{B}x_n y_n \end{aligned} \right\} \quad (12)$$

$$V_P = \begin{pmatrix} A - p + 2(1-A)x - y & -q - x \\ \frac{y}{B} & \frac{x}{B} \end{pmatrix}$$

If characteristic root corresponding to V_P is represented by Λ_1, Λ_2 at P , then

$$\Lambda_1 + \Lambda_2 = 2 + B - AB - p \quad (13)$$

Solving equations (13) and (14) brings out the lines of marginal stability under the following conditions ($\Lambda_1 = \pm 1$ and $\Lambda_1 \Lambda_2 = 1$). The presence of these conditions guarantees that the moduli of the eigenvalues are less than 1.

When $\Lambda_1 \Lambda_2 = 1$, then from (14), we can get

$$M_1 : A + 2B - 2AB - p - \frac{(-1+A)(-1+B)q}{B} - 1 = 0 \quad (15)$$

When $\Lambda_1 = 1$, then from (13) and (14), we can get

$$M_2 : \frac{(-1+A)(-1+B)(B+q)}{B} = 0 \quad (16)$$

When $\Lambda_1 = -1$, then from (13) and (14), we can get

$$M_3 : 3AB + 2p + \frac{(-1+A)(-1+B)q}{B} - 3 - A - 3B = 0 \quad (17)$$

By taking (15), (16) and (17) in conjunction, we obtain the triangular region, which further reveals the fact that $|\Lambda_{1,2}| < 1$.

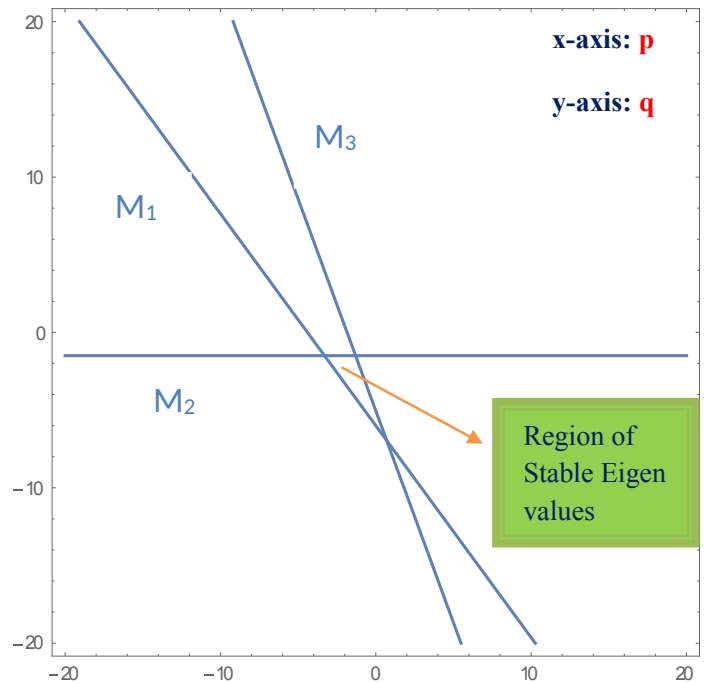


Figure 1 Region of stability where $|\Lambda_{1,2}| < 1$

NUMERICAL SIMULATION

As a follow-up to our theoretical results, here we will provide some numerical simulations to support the dynamical behavior of the system (3). Our results would not be hyperbolic if $B = 0.5$. According to Lemma 2.3, if $A = 2.5$, the bifurcation parameter will be stable. It is however not possible to have a stable bifurcation parameter if $A < 2.5$, as then attracting close curves will emerge from a positive equilibrium. Based on Figures 14 and 25, the local stability of the unique positive equilibrium is ensured. Based on

Figures 15 and 17, one can immediately see from Figure 16 and Figure 18 an attractor of the system (3). As a result, Figure 2 to Figure 13 represent the local stability of the system (3), whereas Figure 14 to Figure 25 illustrate the global asymptotic stability of the unique positive equilibrium. As shown in Figure 20 to Figure 24, the unique positive equilibrium is unstable for different parameter choices when $B < 0.5$, whereas an attracting invariant closed curve bifurcates from the positive equilibrium. Figure 26 and Figure 27 show the Neimark-Sacker bifurcation of the system (3). The state feedback control method is then used to stabilize the chaos in the discrete biological model (3). We now proceed to Section (4) to verify the validity of the results obtained. Suppose $A = 3.2$ and $B = 1.5$, then (15), (16) and (17) can be obtained based on these values

$$M_1 : -4.4 - p - 0.733333q = 0 \tag{18}$$

$$M_2 : 0.733333(1.5 + q) = 0 \tag{19}$$

$$M_3 : 3.7 + 2p + 0.733333q = 0 \tag{20}$$

The lines found in (18), (19) and (20) form a triangle that represents the region encompassing $|\Lambda_{1,2}| < 1$ (see Figure 1). Figure 28 and Figure 29 show that the system (3) is sensitive to their initial conditions, which is a useful indicator of the system's sensitivity. Last but not least, numerical verification was performed to confirm the theoretical results. In different aspects of biology, especially in the field of ecology, this research can provide a theoretical basis for research.

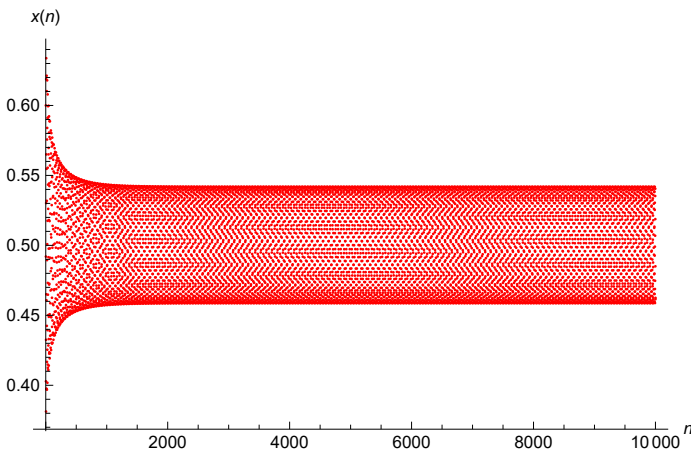


Figure 2 Shows behavior of solution of x_n , when $A = 2.3, B = 0.499, x_0 = 0.6, y_0 = 0.7$

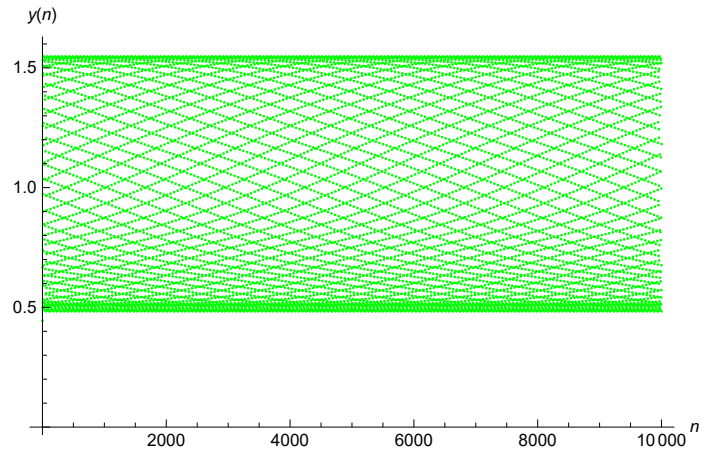


Figure 3 Shows behavior of solution of y_n , when $A = 2.98, B = 0.45, x_0 = 0.4, y_0 = 0.5$

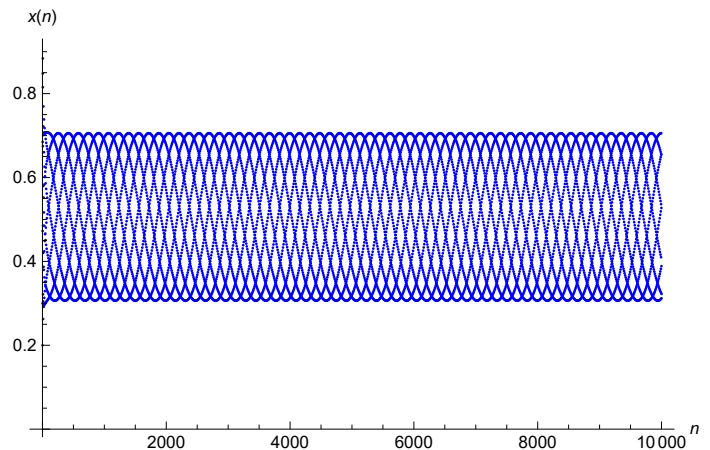


Figure 4 Shows behavior of solution of x_n , when $A = 2, B = 0.48, x_0 = 0.2, y_0 = 0.3$

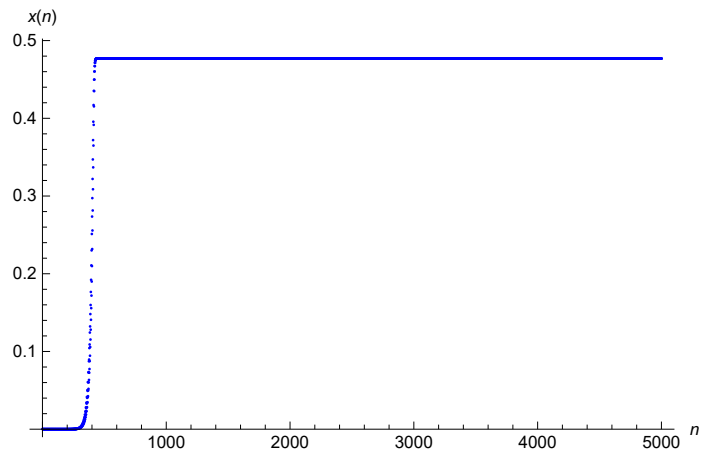


Figure 5 Shows behavior of solution of x_n , when $A = 3.51, B = 0.81, x_0 = 0.003, y_0 = 0.004$

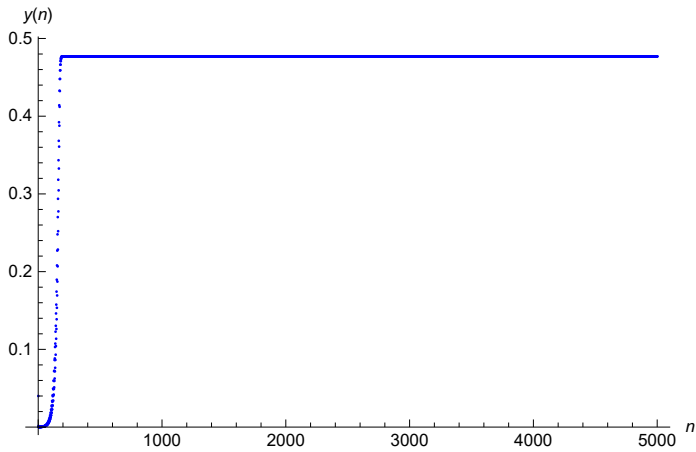


Figure 6 Shows behavior of solution of y_n , when $A = 3.51, B = 0.81, x_0 = 0.03, y_0 = 0.04$

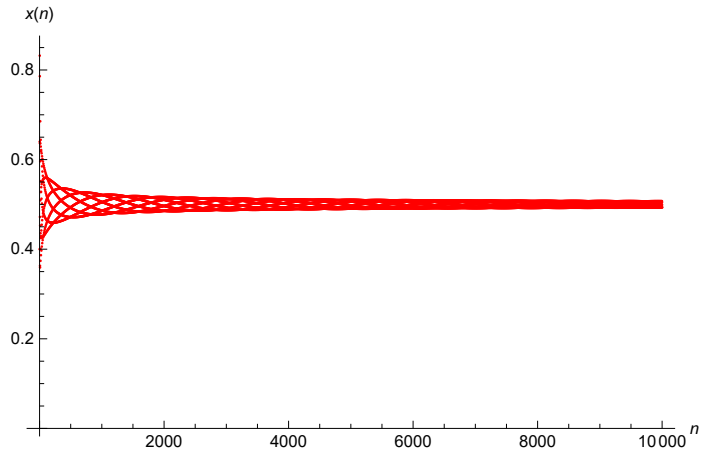


Figure 9 Shows behavior of solution of x_n , when $A = 2.5, B = 0.5, x(0) = 0.4, y_0 = 0.3$

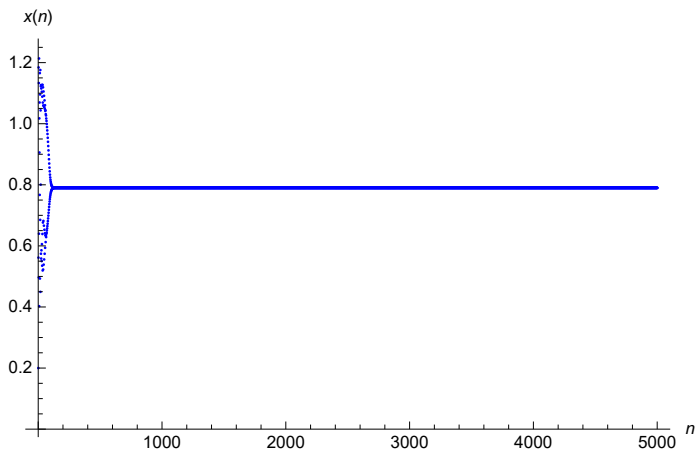


Figure 7 Shows behavior of solution of x_n , when $A = 3.76, B = 0.79, x_0 = 0.2, y_0 = 0.4$

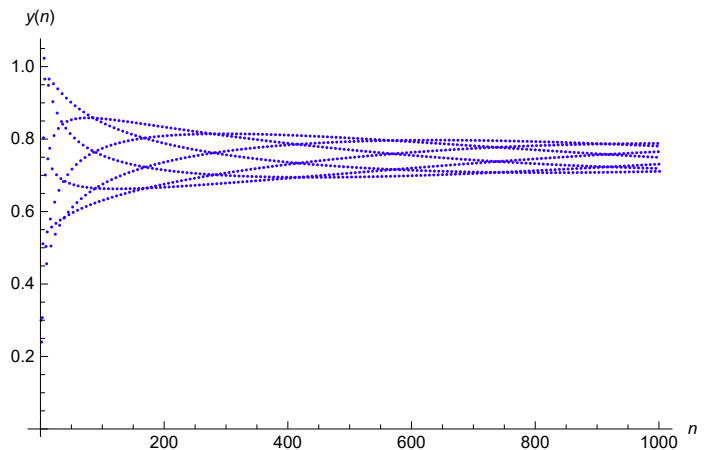


Figure 10 Shows behavior of solution of y_n , when $A = 2.5, B = 0.5, x_0 = 0.4, y_0 = 0.3$

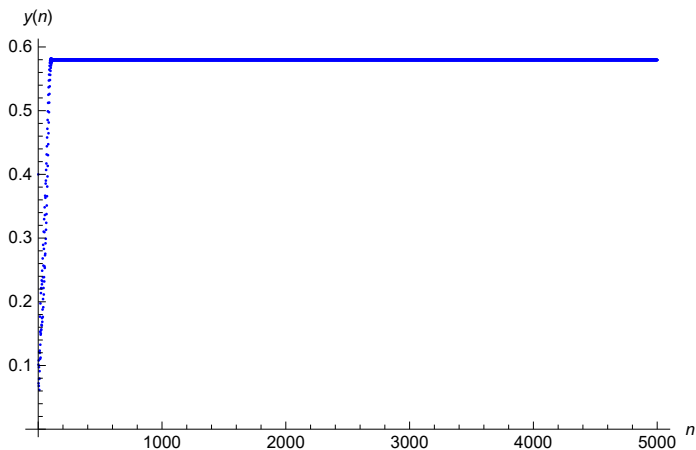


Figure 8 Shows behavior of solution of y_n , when $A = 3.76, B = 0.79, x_0 = 0.2, y_0 = 0.4$

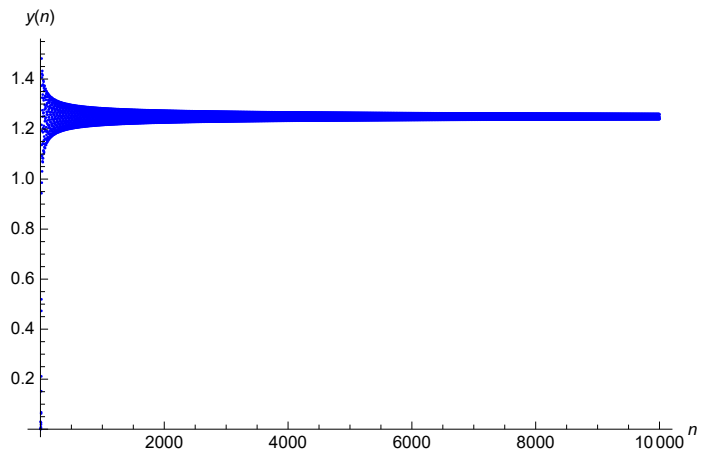


Figure 11 Shows behavior of solution of y_n , when $A = 3.5, B = 0.5, x_0 = 0.04, y_0 = 0.03$

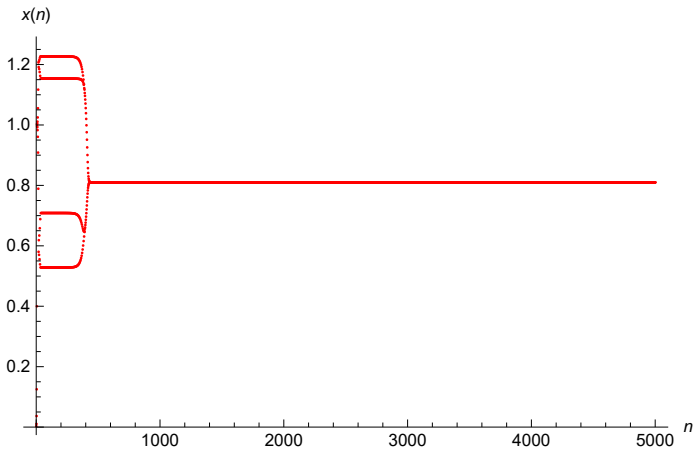


Figure 12 Shows behavior of solution of x_n , when $A = 3.51, B = 0.81, x_0 = 0.003, y_0 = 0.004$

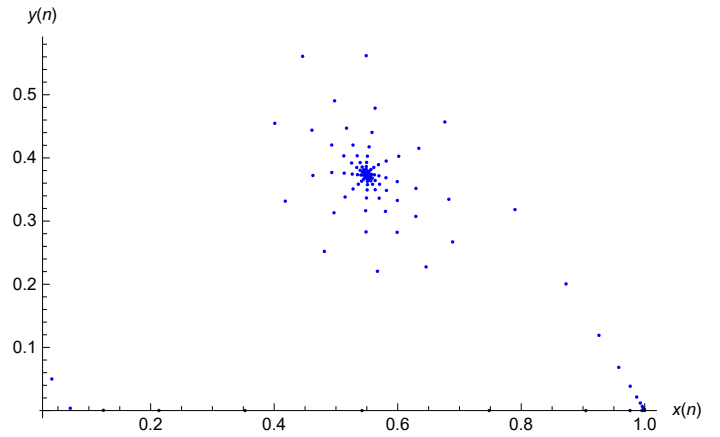


Figure 15 Shows phase portrait in (x, y) plane, when $A = 2.33, B = 0.5, x_0 = 0.003, y_0 = 0.005$, of system (3)

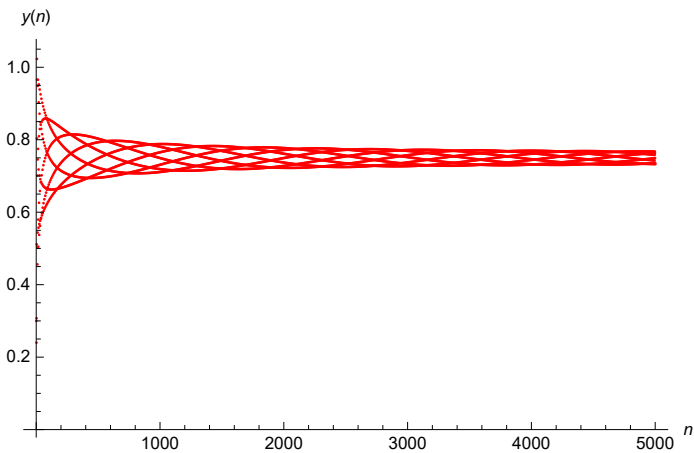


Figure 13 Shows behavior of solution of y_n , when $A = 2.5, B = 0.5, x_0 = 0.4, y_0 = 0.3$

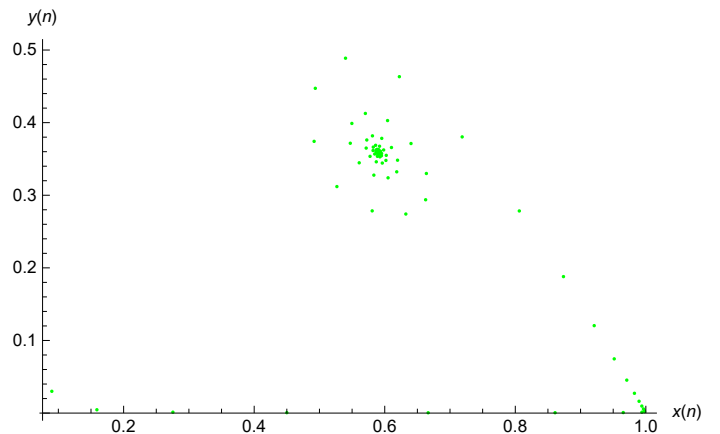


Figure 16 Shows phase portrait in (x, y) plane, when $A = 1.83, B = 0.55, x_0 = 0.04, y_0 = 0.05$, of system (3)

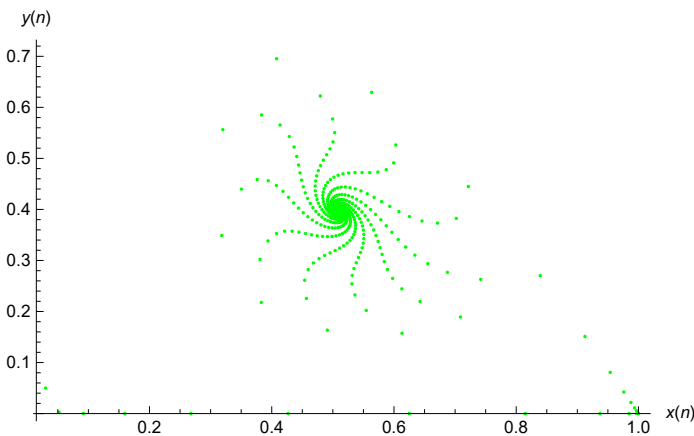


Figure 14 Shows phase portrait in (x, y) plane, when $A = 1.81, B = 0.51, x_0 = 0.03, y_0 = 0.05$, of system (3)

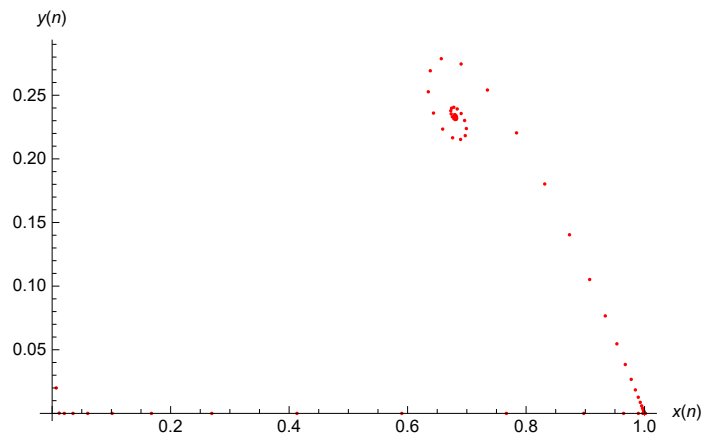


Figure 17 Shows phase portrait in (x, y) plane, when $A = 1.876, B = 0.59, x_0 = 0.09, y_0 = 0.03$, of system (3)

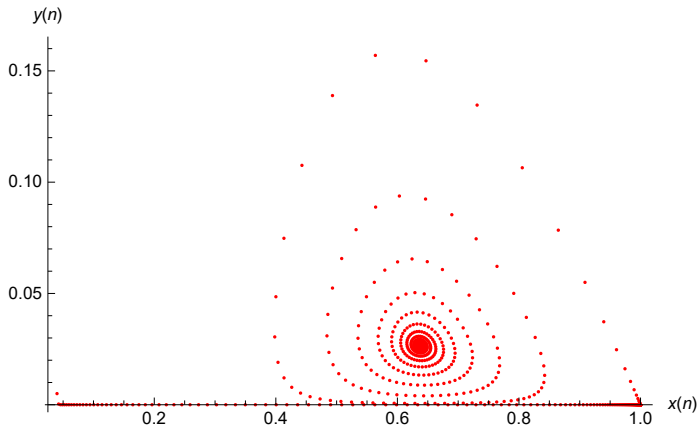


Figure 18 Shows phase portrait in (x, y) plane, when $A = 1.073, B = 0.637, x_0 = 0.04, y_0 = 0.005$, of system (3)

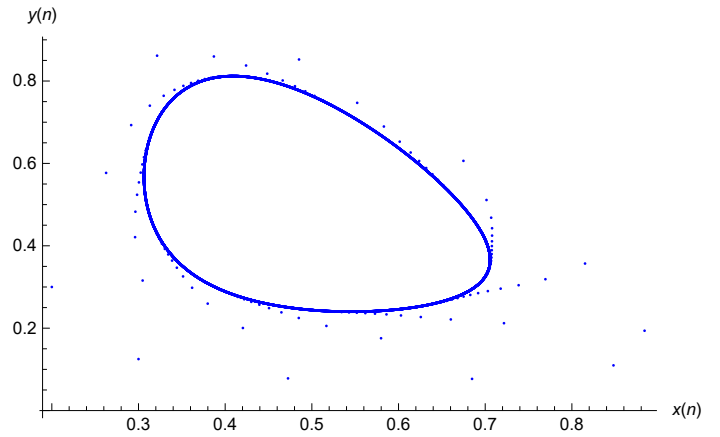


Figure 21 Shows phase portrait in (x, y) plane, when $A = 2, B = 0.48, x_0 = 0.2, y_0 = 0.3$, of system (3)

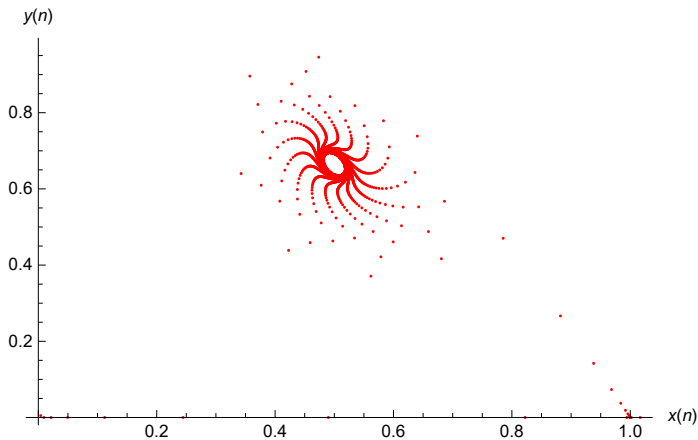


Figure 19 Shows phase portrait in (x, y) plane, when $A = 2.43, B = 0.44, x_0 = 0.0035, y_0 = 0.041$, of system (3)

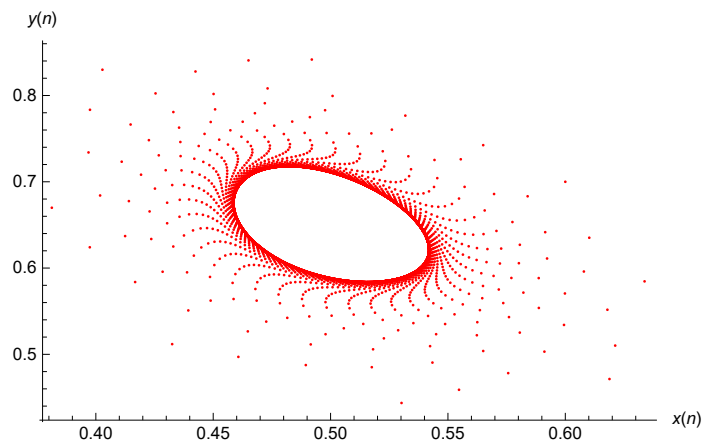


Figure 22 Shows phase portrait in (x, y) plane, when $A = 2.3, B = 0.499, x_0 = 0.6, y_0 = 0.7$, of system (3)

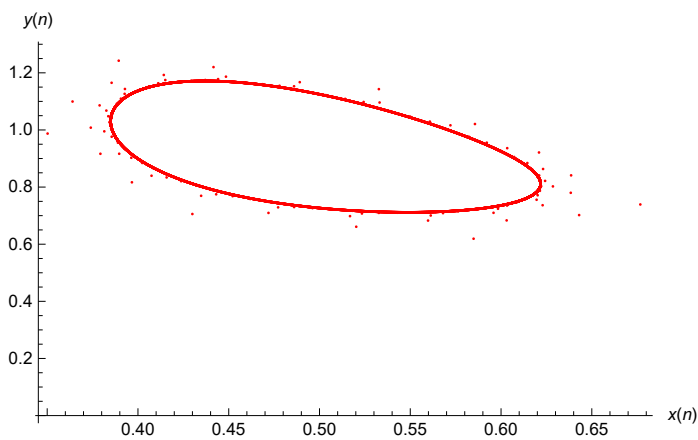


Figure 20 Shows phase portrait in (x, y) plane, when $A = 2.87, B = 0.49, x_0 = 0.7, y_0 = 0.8$, of system (3)

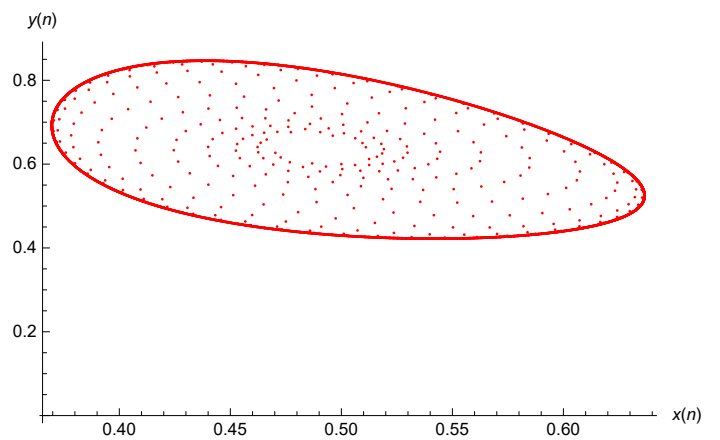


Figure 23 Shows phase portrait in (x, y) plane, when $A = 2.25, B = 0.49, x_0 = 0.5, y_0 = 0.6$, of system (3)

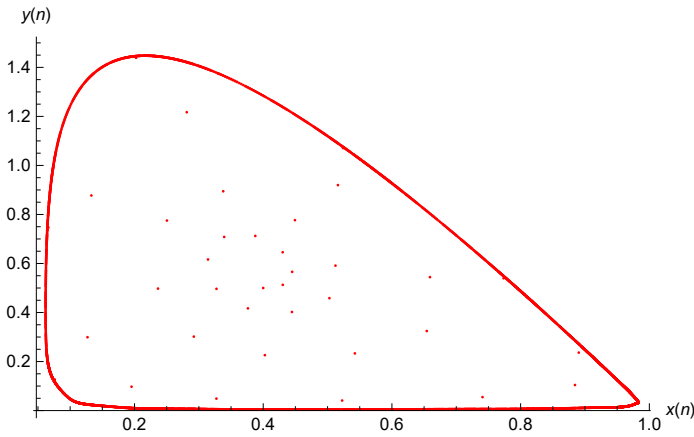


Figure 24 Shows phase portrait in (x, y) plane, when $A = 1.96, B = 0.39, x_0 = 0.4, y_0 = 0.5$, of system (3)

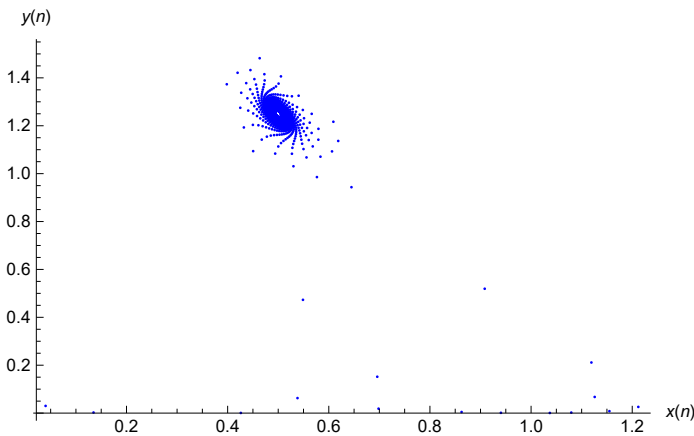


Figure 25 Shows phase portrait in (x, y) plane, when $A = 1.96, B = 0.39, x_0 = 0.4, y_0 = 0.5$, of system (3)

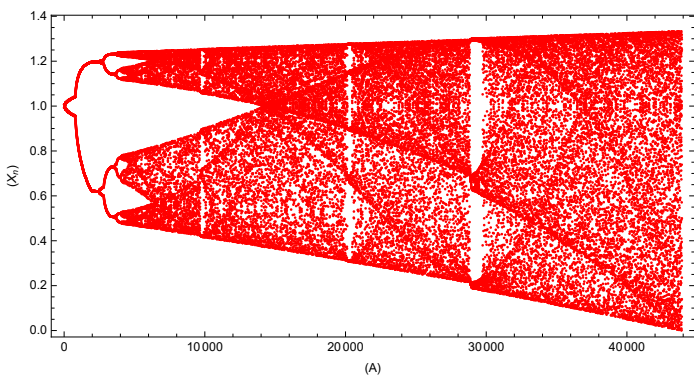


Figure 26 Neimark-Sacker bifurcation diagram of system (3) in (A, x_n) plane

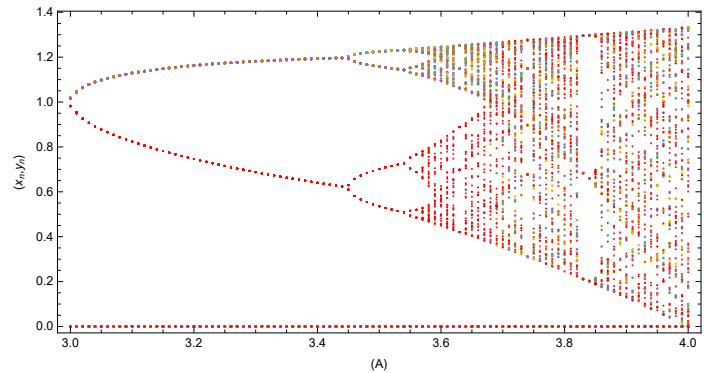


Figure 27 Neimark-Sacker bifurcation diagram of system (3) in (A, y_n) plane

MAXIMUM LYAPUNOV EXPONENT

The Lyapunov exponent is a concept derived from chaos theory and dynamical systems. The aim of this measurement is to determine how sensitive chaotic systems are to their initial conditions. When calculating adjacent trajectory divergences in phase space, one can use the Lyapunov exponent (Abarbanel 1996).

Positive Lyapunov exponents cause the trajectory of a system to diverge exponentially, leading to it being classified as chaotic. When Lyapunov exponents are above zero, the system outcomes are highly sensitive to conditions at the start, indicating even small changes could have major impacts. Alternatively, a negative Lyapunov exponent indicates that nearby trajectories are convergent, which indicates a predictable and stable system. From a mathematical perspective, it is defined as:

Definition 3: For the map

$$\Theta : \mathbb{R} \mapsto \mathbb{R}$$

The Lyapunov exponent is defined as:

$$\tilde{L} = \lim_{n \rightarrow \infty} \ln \left| \frac{d}{dx} \Theta^n(x = x_0) \right|^{\frac{1}{n}} \quad (21)$$

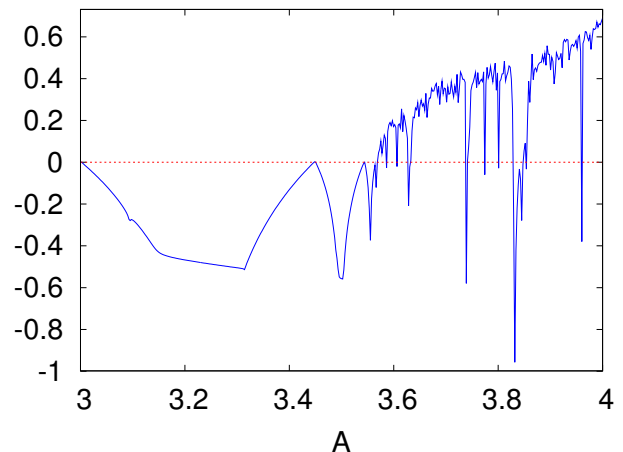


Figure 28 Maximum Lyapunov Exponent of the model (3)

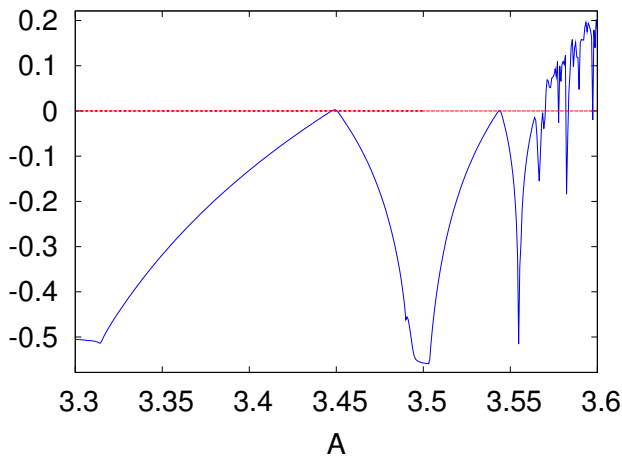


Figure 29 Maximum Lyapunov Exponent of the model (3)

CONCLUSION AND DISCUSSION

Previous research has demonstrated that population models described by difference equations have a crucial role in population dynamics and mathematical ecology. In this study, we examine the qualitative and dynamic properties of discrete predator-prey models. Based on bifurcation theory, we determined the stability conditions for a unique steady state. In this paper, we demonstrate that the model (3) undergoes NS bifurcation. Moreover, we present some numerical simulations including the behavior of solution of prey x_n and predator y_n over time (n), phase portraits of system by taking different initial conditions and the values of parameters and the bifurcation diagram determining the range of the bifurcation parameter ($3 < A < 4$). All this numerical study has been conducted by using "Mathematica" program which verify our theoretical results.

In this paper, we demonstrate that the stability of the unique fixed point (3) occurs at a critical bifurcation value when the bifurcation parameter (A) reaches this critical value. Neimark-Sacker bifurcation follows. A more complex dynamics is also visible in certain regions in the model (3) when the parameter values are changed. We can conclude that parameter (A) is highly important for the stability of model (3). Additionally, under the influence of the Neimark-Sacker bifurcation, invariant closed curves are dynamically unstable. Model (3) is an interaction between predators and prey that can be viewed from the perspective of biology. As a result, both prey and predator populations are capable of oscillating around some mean values under suitable conditions since NS bifurcation exists in the model (3). In addition, the chaotic behavior of the model (3) can be controlled by using feedback control techniques. Besides showing the MLE, the article concludes that the system fluctuates within the chaotic region.

Availability of data and material

Not applicable.

Conflicts of interest

The authors declare that there is no conflict of interest regarding the publication of this paper.

LITERATURE CITED

- Abarbanel, H. D. I., 1996 *Analysis of Observed Chaotic Data*. Number 34, Springer New York, NY.
- Alaydi, S., 1996 *An introduction to difference equations*. Number 32, Springer New York, NY.
- Chen, Y. and S. Changming, 2008 Stability and hopf bifurcation analysis in a prey-predator system with stage-structure for prey and time delay. *Chaos, Solitons & Fractals* **38**: 1104–1114.
- Fazly, M. and M. Hesaaraki, 2007 Periodic solutions for a discrete time predator-prey system with monotone functional responses. *Comptes Rendus. Mathématique* **345**: 199–202.
- Gakkhar, S. and A. Singh, 2012 Complex dynamics in a prey predator system with multiple delays. *Communications in Nonlinear Science and Numerical Simulation* **17**: 914–929.
- Garic Demirovic M., K. M. . N. M., 2009 Global behavior of four competitive rational systems of difference equations in the plane. *Discrete Dynamics in Nature and Society* **2009**: 153058–153092.
- Hu Z., T. Z. . Z., 2011 Stability and bifurcation analysis of a discrete predator-prey model with nonmonotonic functional response. *Nonlinear Analysis: Real World Applications* **12(4)**: 2356–2377.
- Ibrahim, T. F. and N. Touafek, 2014 Max-type system of difference equations with positive two-periodic sequences. *Math. methods Appl. sci* **37**: 2562–2569.
- Joydip Dhar, H. S. . H. S. B., 2015 Discrete-time dynamics of a system with crowding effect and predator partially dependent on prey. *Applied Mathematics and Computation* **252**: 1104–1114.
- Kalabusic S., K. M. . P. E., 2011 Multiple attractors for a competitive system of rational difference equations in the plane. *Abstract and Applied Analysis* **37(16)**: 1–17.
- Khan, A., 2016 Neimark-Sacker bifurcation of a two-dimensional discrete-time predator-prey model. *SpringerPlus* **5**: 121–126.
- L. Men, G. W. Z. W. L. . W. L., B. S. Chen, 2015 Hopf bifurcation and nonlinear state feedback control for a modified Lotka-Volterra differential algebraic predator-prey system. *Fifth International Conference on Intelligent Control and Information Processing* **2015**: 233–238.
- Pan, S. X., 2013 Asymptotic spreading in a Lotka-Volterra predator-prey system. *The Journal of Mathematical Analysis and Applications* **407**: 230–236.
- Q., Q. M. . K. A., 2015 Periodic solutions for discrete time predator-prey system with monotone functional responses. *International Academy of Ecology and Environmental Sciences* **5(1)**: 48–62.
- R. M. Eide, N. T. F. . R. A. V. G., A. L. Krause, 2018 The origins and evolutions of predator-prey theory. *Journal of Theoretical Biology* **451**: 19–34.
- Rana, S., U. Kulsum, *et al.*, 2017 Bifurcation analysis and chaos control in a discrete-time predator-prey system of leslie type with simplified holling type iv functional response. *Discrete Dynamics in Nature and Society* **2017**.
- Salman SM, Y. A. . E. A., 2016 Stability, bifurcation analysis and chaos control of a discrete predator-prey system with square root functional response. *Chaos Solitons Fractals* **93**: 20–31.
- Sen M, B. M. . M. A., 2012 Bifurcation analysis of a ratio-dependent prey-predator model with the Allee effect. *Ecological Complexity* **11**: 12–27.
- Singh, A. and P. Deolia, 2020 Dynamical analysis and chaos control in discrete-time prey-predator model. *Communications in Nonlinear Science and Numerical Simulation* **90**: 105313.
- Smith, J. M., 1968 *Mathematical Ideas in Biology*, volume 1. Cambridge University Press.
- X. W. Jiang, T. W. H. . H. C. Y., X. Y. Chen, 2021 Bifurcation and control for a predator-prey system with two delays. *IEEE Trans-*

- actions on Circuits and Systems II: Express Briefs **68**: 376–380.
- X. Zhang, Z. W. . T. Z., 2016 Periodic solutions for discrete time predator-prey system with monotone functional responses. *Journal of Biological Dynamics* **10**: 1–17.
- Z. L. Luo, Y. P. L. . Y. X. D., 2016 Rank one chaos in periodically kicked Lotka-Volterra predator-prey system with time delay. *Nonlinear Dynamics* **85**: 797–811.
- Zhang C.H, Y. X. . C. G., 2010 Hopf bifurcations in a predator-prey system with a discrete delay and a distributed delay. *Nonlinear Anal Real World Application* **10**: 4141–4153.
- Zu, L., D. Jiang, D. O'Regan, T. Hayat, and B. Ahmad, 2018 Ergodic property of a lotka-volterra predator-prey model with white noise higher order perturbation under regime switching. *Applied Mathematics and Computation* **330**: 93–102.

How to cite this article: Abbas, A., and Khaliq, A. Analyzing Predator-Prey Interaction in Chaotic and Bifurcating Environments. *Chaos Theory and Applications*, 5(3), 207-218, 2023.

Licensing Policy: The published articles in *Chaos Theory and Applications* are licensed under a [Creative Commons Attribution-NonCommercial 4.0 International License](#).

